crystals

MDPI

Article

Influence of Sheet Thickness and Process Parameters on the Microstructure and Mechanical Properties of Brazed Welding Used for Cold-Formed Steel Beams

Iosif Hulka [1], Viorel Ungureanu [2,3,*], Silviu Saraolu [2], Alin Popescu [2] and Alexandru Pascu [4]

[1] Research Institute for Renewable Energies, Politehnica University Timişoara, G. Muzicescu 138, 300501 Timişoara, Romania; iosif.hulka@upt.ro
[2] Department of Steel Structures and Structural Mechanics, Politehnica University Timişoara, Ioan Curea 1, 300224 Timişoara, Romania; saraolu.silviu@gmail.com (S.S.); popescu_alin91@yahoo.ro (A.P.)
[3] Romanian Academy, Timişoara Branch, Mihai Viteazu 24, 300223 Timişoara, Romania
[4] Materials Engineering and Welding Department, Transilvania University of Braşov, Eroilor 29, 500036 Brasov, Romania; alexandru.pascu@unitbv.ro
* Correspondence: viorel.ungureanu@upt.ro

Abstract: Metal inert gas (MIG) brazing was used to join galvanized thin sheets with thicknesses in the range of 0.8 to 2 mm in a lap joint configuration using $CuAl_8$ wire as filler. The process was used to manufacture built-up cold-formed steel beams composed of corrugated steel webs and flanges made from thin-walled cold-formed steel lipped channel profiles. The effect of heat input and sheet thickness on joint properties, such as macro- and microstructure, wettability, and mechanical characteristics such as microhardness and tensile strength were investigated. The bead geometry was assessed by studying the wettability of the filler material. The microstructure was investigated by digital and scanning electron microscopy, and the composition in the heat-affected zone (HAZ), interface, and bead was determined by energy dispersive spectroscopy. Formation of Fe–Al intermetallics was observed in the bead at the bead–base material interface. Some pores were noticed that formed due to the evaporation of the zinc coating. The bead shape and mechanical properties were found to be the best when 1.2 and 2 mm sheets were brazed using a heat input of 121.4 J/mm. This suggests that not only the heat input but also the thickness of the sheet metal play a crucial role in the production of MIG brazed joints.

Keywords: MIG; brazing; cold-formed steel beams; microstructure; mechanical properties

Academic Editors: Ali Khalfallah and Reza Beygi

Received: 8 March 2025
Revised: 4 April 2025
Accepted: 10 April 2025
Published: 12 April 2025

Citation: Hulka, I.; Ungureanu, V.; Saraolu, S.; Popescu, A.; Pascu, A. Influence of Sheet Thickness and Process Parameters on the Microstructure and Mechanical Properties of Brazed Welding Used for Cold-Formed Steel Beams. *Crystals* **2025**, *15*, 354. https://doi.org/10.3390/cryst15040354

1. Introduction

Trapezoidal corrugated webs are used in the manufacture of steel beams, which are relatively new construction elements that are used as primary structural systems in buildings and bridges. One of the main advantages of this system is the effect of corrugation stability, which increases buckling resistance. The use of thinner steel sheets results in lower costs, making them more economically advantageous. During the manufacturing process, the flanges, which provide the main resistance to bending, are made of flat sheets welded to trapezoidal or sinusoidal sheets of the web using a specific joining method [1]. One of these methods is the resistance spot welding process (RSW), which was investigated as an alternative technique to self-drilling screws to join components of built-up beams [2], but the method was found to increase stiffness and reduce ductility. After reaching the maximum force during the tests, the failure mechanism was attributed to distortion of the web corrugation along spot weld failures [3].

However, RSW is one of the most used processes in the automotive industry because of its efficiency to join a wide range of materials and thicknesses [4].

During RSW, degradation of the electrode occurs caused by the formation of Cu–Zn compounds at the tip and within the base material, causing the joint to form unpredictably [5]. Joining thin galvanized steel sheets has become more significant in the industry but requires considerable control of heat input to lower thermal distortion and reduce zinc loss in the vicinity of the joint [6].

Conventional welding processes such as laser welding or tungsten inert gas welding cannot be used for joining steel sheets due to the higher heat input generated by these processes. In this regard, metal inert gas (MIG) brazing is a promising method to join thin zinc galvanized sheets due to advantages such as better stability, good deposition rate and lower heat input [7].

Based on its use in the automotive industry, it has been found to be an effective process to improve the performance of web corrugation.

MIG brazing is a non-fusion process that occurs at lower temperatures than other welding methods, causing a smaller heat-affected zone (HAZ). The wire electrodes used in brazing melt at temperatures below 1000 °C, which is beneficial for joining steel sheets that are generally heat-sensitive, or for joining dissimilar metals [8]. Moreover, due to the smaller HAZ, less zinc is burnt away when galvanized steel sheets are used, and the method offers better control over the formation of brittle phases [9].

Chovet and Guiheux used MIG brazing to join 1–2 mm thick ferritic sheets for automotive applications using $CuAl_8$, $CuAl9Ni_5Fe_3Mn_2$ and $CuMn13Al_7$ wires as fillers. They concluded that the method was more efficient compared to other welding processes because the low heat input helped to reduce the width of the heat-affected zone (HAZ) and limited the degradation of the Zn coating to the surrounding area of the bead only [10]. Basak et al. successfully joined galvanized dual-phase steel sheets using MIG brazing with CuAl filler and found that the bead geometry is directly affected by the process parameters and operating mode, which is critical for joint performance [11]. Khan et al. used a Si–bronze filler when brazing DP600 steel sheets using the MIG process, emphasizing the effect of the Zn coating on the strength of the lap joints [12]. Generally, galvanized steel sheets such as High Strength Steel (HSS) and Advanced High Strength Steel (AHSS) are used in the automotive industry and are joined by MIG brazing using various types of filler materials such as $CuAl_8$, $CuAl_{10}$, $CuSi_3Mn_1$ and $CuSi_3$ [13].

As MIG brazing is generally used in the automotive industry and is of great interest to researchers, the challenge is to adapt and optimize the process to make it suitable to produce lightweight steel structural systems in the construction sector. However, it is known that the brazed joints have a direct influence on the fatigue strength since they act as metallurgical and structural discontinuities which can become starting points of joint failure [14].

In this regard, it is still a challenge to achieve MIG-brazed defect-free joints with improved mechanical properties due to the formation of defects within the bead.

The present study aims to further investigate the technical solution proposed by the WELLFORMED research project implemented by the CEMSIG Research Centre of the Politehnica University Timisoara. The project proposed MIG brazing as a new joining solution for cold-formed steel beams made entirely from corrugated steel webs and flanges made from thin-walled cold-formed profiles. Therefore, this study aims to comprehensively analyze the effect of steel sheet thickness and process parameters on the microstructural characteristics of MIG brazed joints, using $CuAl_8$ wire as the filler material. In addition, the investigation includes the evaluation of mechanical properties, including Vickers hardness

and tensile strength, to determine the relationship between heat input, sheet thickness, joint microstructure and their performance.

2. Materials and Methods

The present study used a MEGAPULS FOCUS 330 welding machine (Rehm GmbH u. Co. KG Schweißtechnik, Uhingen, Germany) equipped with a TBI XP 363S welding torch. Brazing was carried out using the MIG CC+ process with a 1 mm diameter $CuAl_8$ wire and a manually operated torch with the parameters presented in Table 1.

Table 1. Annotation and brazing parameters.

	T1 [mm]	**T2 [mm]**	**I [A]**	**Ua [V]**	**Protecting Gas Argon 4.6 [L/min]**	**Torch Tilting [°]**
Specimen 1	0.8	2	120	14.3	14–16	15–20
Specimen 2	1	2	130	14.7		
Specimen 3	1.2	2	140	15.3		

During the process, an electric arc is created between the $CuAl_8$ wire electrode and the base material. The electrode is pulled from a coil mounted on a wire feeder driven by a motor and pushed through the welding torch hose up to the contact tips. The positive pole is connected to the wire electrode, and the negative pole is connected to the base material. The arc formed between the $CuAl_8$ electrode and the base materials melts the wire and, to some extent, the base material. The wire electrode is therefore the conductor for the arc and the brazing filler material. Cold-rolled S250 GD grade galvanized thin sheets ranging from 0.8 to 2 mm thickness were used to prepare the specimens. The chemical composition of the commercial sheets, ranging from 0.8 to 1.2 mm, used in this study is C $\leq$ 0.2 wt.%, Si $\leq$ 0.6 wt.%, Mn $\leq$ 1.7 wt.%, P $\leq$ 0.1 wt.% and S $\leq$ 0.045 wt.%. According to the manufacturer, the 2 mm thick sheet used was an S3560 GD grade with a chemical composition similar to S250GD.

Metallographic specimens of the brazing joints were cut using a liquid-cooled cutting machine to avoid overheating and microstructural changes. After cutting, the specimens were embedded in epoxy resin and ground using SiC abrasive papers of various grits up to P4000 followed by polishing using adhesive polished cloths in the range of $9 - 1$ µm, using diamond suspension with grain sizes of 1 µm at the final stage. To reveal the microstructure, Nital was used as an etchant at a concentration of 5% for the base material and Klemm's reagent for the bead. A laser confocal microscope (OLS 4000 LEXT, Olympus, Tokio, Japan) and a field emission scanning electron microscope (SEM, Quanta FEG 250, FEI, Hillsboro, OR, USA) were used to observe the macro- and microstructure of the joints in the cross-section. The chemical analysis of different regions of the cross-section of the samples was studied by energy dispersive spectroscopy (EDX, Apollo SSD detector, EDAX Inc., Mahwah, NJ, USA).

Mechanical properties were determined by Vickers measurements and tensile tests. The microhardness of the specimens was measured using an automated Vickers microhardness tester (FALCON 600G2, INNOVATEST Europe BV, Maastricht, The Netherlands). Indentations were made on the cross-section of each sample using a load of 200 gf and a dwell time of 15 s.

Since a full-scale beam consists of joining various thinner web plates to thicker flanges or shear plates, lap joint specimens were tested to assess their response to mechanical loading. The design of the tensile test specimens is shown in Figure 1, where the dimensions of the plates are given. The specimens were fabricated in a lap position with an overlap

of 50 mm and both sides of the overlapping plates were welded. Experimental tests were carried out on a universal testing machine (1000SP, ZwickRoell GmbH & Co. KG, Ulm, Germany) with the load monitored by the machine's load cell and strain monitored by an extensometer with a distance of 80 mm between the sensors.

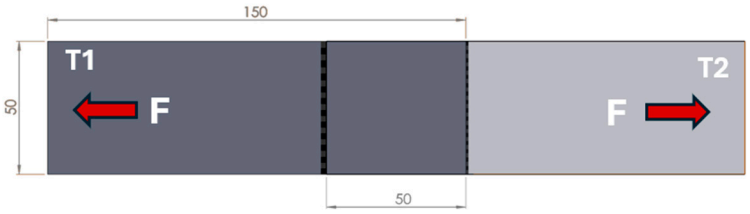

Figure 1. Design of tensile test specimen in which T1 is the thinner member (0.8, 1, 1.2 mm) and T2 is the thicker member (2 mm) with an overlap of 50 mm. The arrows indicate the direction of the applied forces (F).

3. Results and Discussions

3.1. Macro- and Microstructural Observations

Figure 2 shows cross-sectional macro images of brazed joints produced with different sheet thicknesses and varying heat input where the base material, HAZ and deposited filler are exposed by the etchant. Some contamination can also be seen on the surface of Samples 1 and 2. Pores or narrow areas where the resin cannot penetrate trap suspension and etchant, which are pushed out by compressed air as the samples dry, contaminating the surface to some extent. In addition, some darker areas may correspond to over-etched areas. Calculating the heat input based on the formula presented by Singh et al. [15] with a process efficiency of 0.85 for MIG brazing and an estimated brazing speed of 250 mm/min, the following values were obtained: (i) 97.3 J/mm for Specimen 1; (ii) 108.2 J/mm for Specimen 2; and 121.4 J/mm for Specimen 3. It can be seen from the macro-sections that no significant amount of base material has been melted during the brazing process. The quality of brazed joints improves from Specimen 1 to Specimen 3, with the best wetting observed for Specimen 3. No visible pores or cracks were observed in Specimen 1. The brazed area appears well-formed, but the thinner sheet was more sensitive to overheating. A clear pore can be seen in Specimen 2, most likely caused by zinc evaporation and the deformed thin sheet indicates localized overheating. However, compared to Specimen 1, the 1 mm sheet can tolerate a higher heat input. Specimen 3 shows a well-formed brazed area with no visible defects within the bead. Due to the 1.2 mm sheet thickness and higher heat input, it is likely to have better heat absorption and less risk of overheating which improves wetting with an evenly spread filler material. As can be observed, the wetting angles for all samples in contact with the thinner sheet are below 90°, indicating that the filler material spreads effectively and adheres to the base material. However, according to Sharma et al., the contact angle should be below 90° and should be as low as possible to ensure the best wetting performance [16]. From the micrograph, the contact angle between the filler material and the thinner sheet was calculated and the results are as follows: Specimen 1—29.52°, Specimen 2—58.75°, and Specimen 3—65.48°. Theoretically, Specimen 1 should have a better performance, followed by Specimens 2 and 3. However, it appears that sheet thickness and heat input strongly influence the performance of brazed joints, not to mention that the brazing was done manually. In this case, it is difficult to predict the performance of the brazed bead from the contact angle values. Based on the macrographs, it appears that Specimen 3 has fewer visible defects with a uniform and well-formed bead due to the optimum process parameters selected for the thicker sheets resulting in better heat distribution and wetting of the filler material.

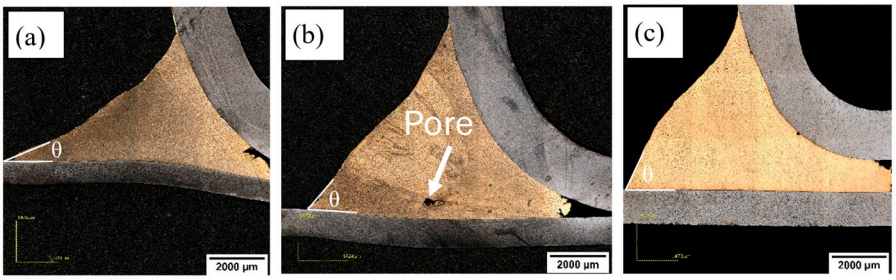

Figure 2. Macro-section of bead shape of the brazed joints at different heat inputs with measured contact angles: 97.3 J/mm and 29.52° for Specimen 1 (**a**), 108.2 J/mm and 58.75° for Specimen 2 (**b**) and 121.4 J/mm and 65.48° for Specimen 3 (**c**).

Figure 3 shows the microstructure at the interface between the base materials and the deposited bead, and the microstructure analyzed in the center of the bead. Analyzing the micrographs, it can be seen that the microstructure of the bead varies depending on the heat input. Additionally, due to the sheet thickness, the alloy experienced different cooling rates.

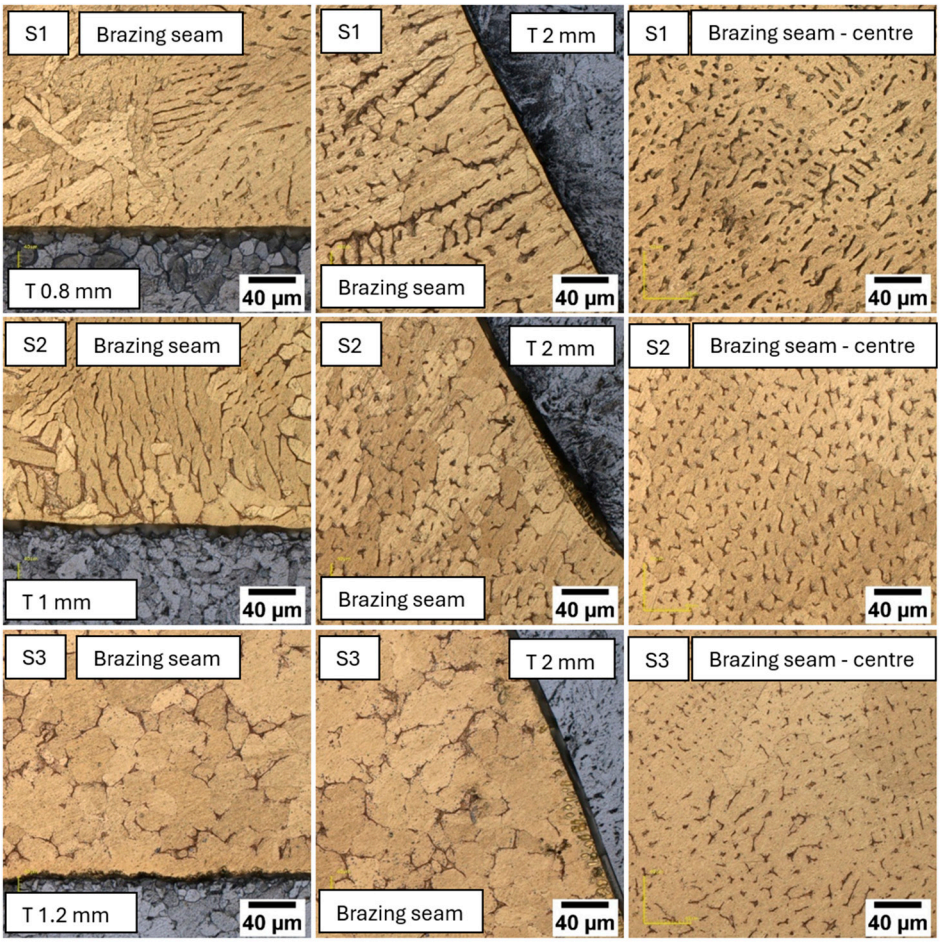

Figure 3. Microstructure at the interface: thin sheet (0.8, 1, and 1.2 mm)—bead interface (**left column**); thick sheet (2 mm)—bead interface (**middle column**), and microstructure of the bead (**right column**); annotation: S1—Specimen 1, S2—Specimen 2, and S3—Specimen 3.

All micrographs were taken at the same magnification, and a heterogeneous structure can be observed, with variations in the shape and size of the grains. In the case of Specimen 1, the microstructure is fine, with randomly oriented elongated grains, suggesting fast directional cooling of the melted $CuAl_8$ filler. Specimen 2 has a coarser structure character-

ized by elongated grains, indicating a slightly slower cooling rate compared to Specimen 1. Specimen 3 has a heterogeneous granular microstructure consisting mainly of equiaxed grains, which is the result of a slow cooling process of the molten $CuAl_8$ filler. It is likely that the thicker sheets cool down more slowly, which is why the grain size has increased. In the center of the bead, in all samples, a biphasic structure can be observed with a different distribution ratio of two phases depending on the solidification rate of the alloy.

During the brazing process, iron diffuses from the surface of the sheets, which is the only source of Fe, resulting in an iron enrichment of the bead, as can be seen from the representative micrograph in Figure 4, areas 1 and 2, and the EDX spectra and quantification. Yu et al. reported similar observations when studying galvanized steel joints brazed using a $CuSi_3$ filler, where iron enriched the fusion zone due to the anode-spot behavior of the arc [17]. Area 1 represents the primary α-Cu matrix with intermetallic phases. Area 2 shows dendrites in which Cu, Al and Fe were identified. Reisgen et al. described that these elements, during brazing, form $Fe_3Al_yCu_z$ intermetallic phases [18], which follow the microstructural and EDX analysis. Considering the amount of Fe identified by EDX, it is more likely that Fe and Al dominate the intermetallic phase at the interface. Basak et al. found that at the interface, Al reacts with Fe, leading to the formation of hard and brittle intermetallic FeAl compounds [11]. As the energy input was gradually increased, the amount of molten base material also increased, which resulted in increased intermetallics formation within the bead near the interface. The amount of these intermetallic phases generally increases with higher heat input [15]. The HAZ (Area 3) reveals a dominant iron peak in the EDX spectra. This indicates the presence of ferrite as the primary microstructural constituent. No traces of zinc were found in any of the samples, suggesting that the heat input caused localized evaporation of the zinc coating.

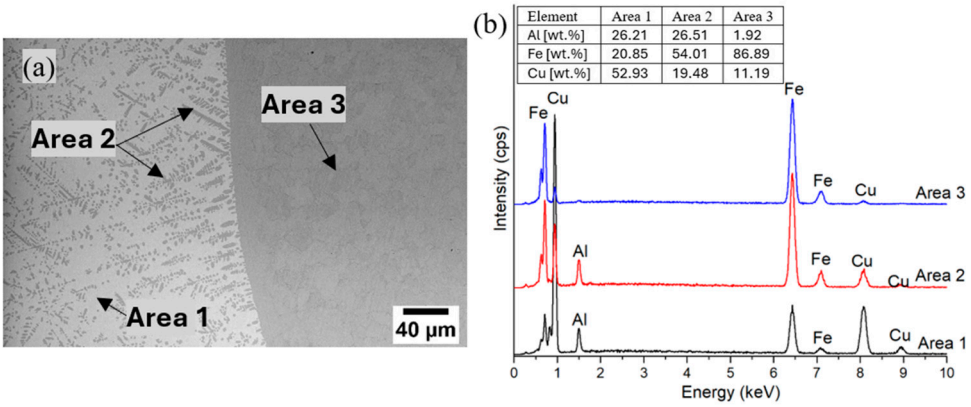

Figure 4. Representative micrograph presenting the intermetallic phases at the base material–bead interface (**a**) and chemical composition of base material and bead near the interface (**b**).

The microstructure of the fusion zones between the bead and thin sheets (0.8–1.2 mm) is presented in Figure 5. The microstructure of the bead at the interface consists of α-dendrites (bright areas) surrounded by eutectic material (grey areas). The presence of dark areas within the bead indicates that Fe from the base material has dissolved into the bead. This is due to the heat input, which caused melting of the base material. The presence of Al as an alloying element in the $CuAl_8$ filler accelerates the reaction with the dissolved Fe atoms within the bead. This reaction is limited by the solubility of Fe in Al, leading to the formation of dendritic intermetallic compounds formed in the bead at the interface [13]. The formation of intermetallics closer to the base material may be attributed to iron's strong affinity for Al rather than Cu, which facilitates the diffusion of Al towards the base material [19]. It might be noted that very fine spherical precipitates (dark points) were also formed during cooling. The presence of Fe promotes the formation of precipitates

distributed throughout the bead and acts as a grain refiner during solidification, which leads to enhanced mechanical properties [18].

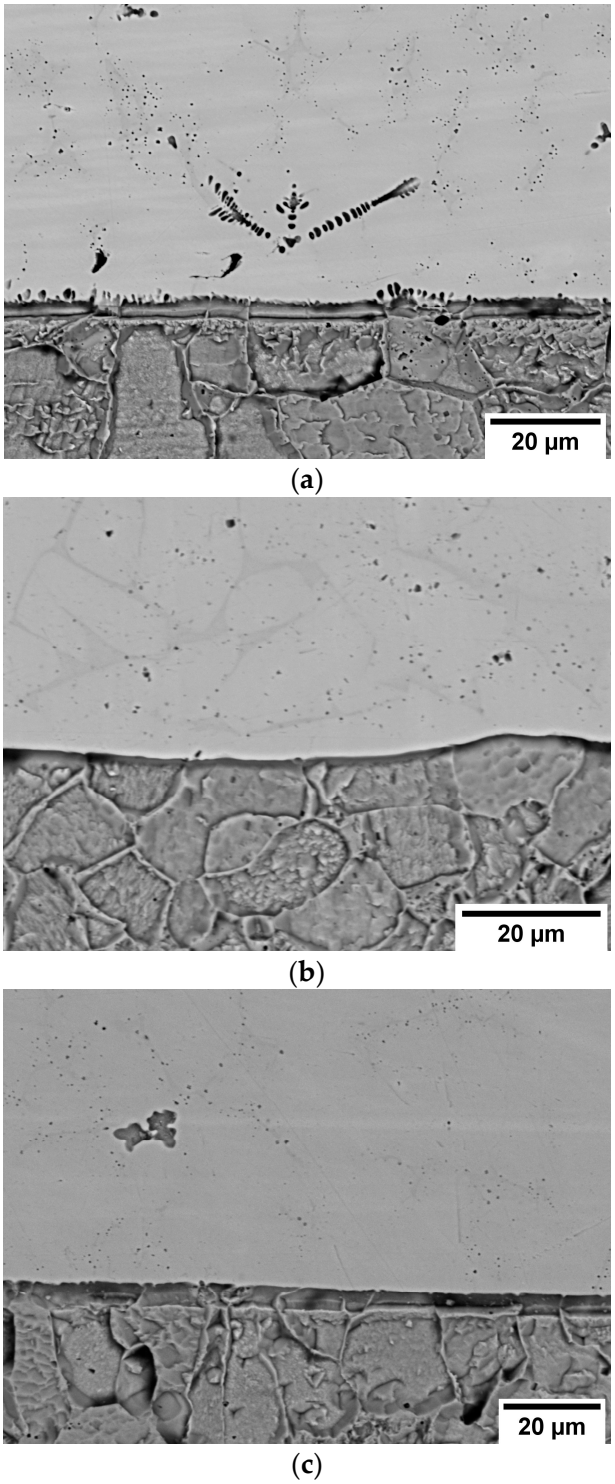

Figure 5. SEM of thin sheets—bead interface (**a**) S 1 T 08 mm, (**b**) T 1 mm and (**c**) T 1.2 mm.

According to the EDX line scans presented in Figure 6, collected from the thin sheets HAZ and the bead interface, it can be seen that needle-like and fine spherical precipitates are rich in Fe. Based on the investigation, there is no clear evidence that Cu was present in the base material. It was observed that the issue of Cu penetration in the base material at grain boundaries is more common in the case of pure Cu filler, as described by Singh et. al. [20].

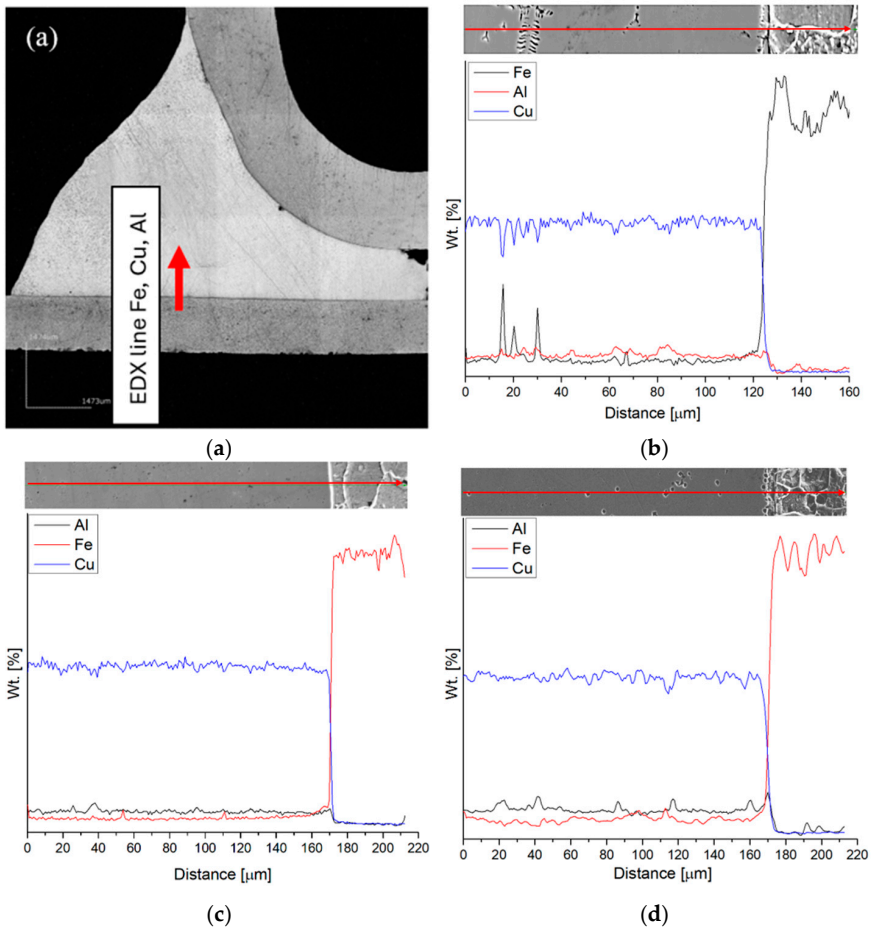

Figure 6. Representative brazed joint indicating EDX scan direction performed at the interface starting in the bead and ending in HAZ (**a**), and EDX of thin sheets—bead interface (**b**) S 1 T 08 mm, (**c**) T 1 mm and (**d**) T 1.2 mm. The EDX line scan was performed at the interface starting in the bead and ending in HAZ as described by the arrows in the associated micrographs.

Compared to the interface, the center of the bead in all samples is characterized by α-Cu solid solution with Al and traces of Fe in its matrix, as shown in Figure 7, Area 2. The amount of Fe is significantly lower compared to the areas examined near the interface, suggesting that the likelihood of new Fe-based phase formation is reduced. Area 1, however, shows a slightly higher concentration of Fe, compared to Area 2, which, due to its higher atomic number, appears as darker grey areas in the micrograph, which is also supported by the EDX investigation.

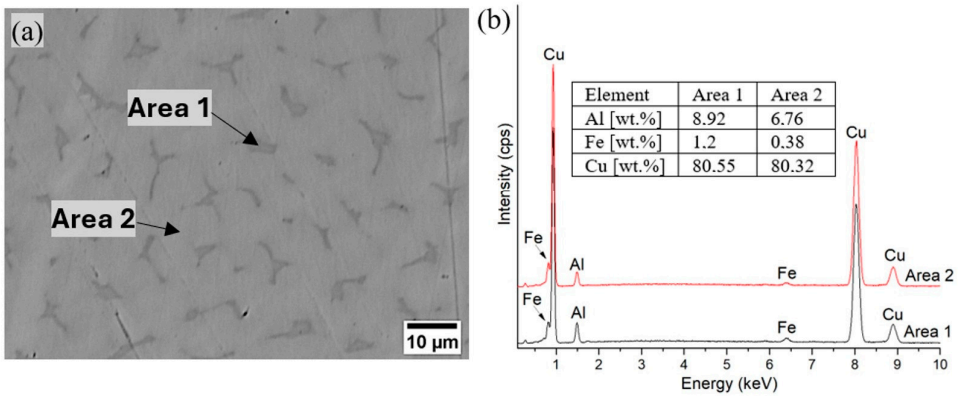

Figure 7. Representative bead microstructure (**a**) and chemical composition (**b**).

3.2. Mechanical Properties

To investigate the microhardness distribution of the studied specimens, eight measurements were performed at each interface (distributed in two directions: 1—thicker sheet and bead interface and 2—thinner sheet and bead interface) and nine measurements were taken in the center of the bead, as described in Figure 8.

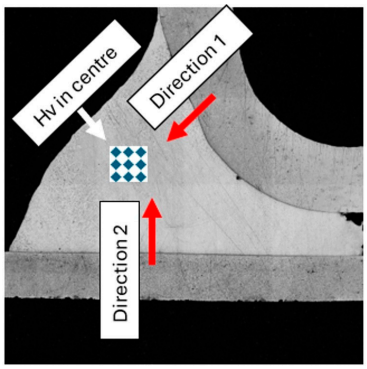

Figure 8. Hardness measurements in areas of interest.

The hardness values for the sheets used in the study were presented in [21] where, according to their measurements, the hardness of the sheets increased with thickness. Hardness measurements (HV_{01}), carried out with a distance of 250 µm between indentations, showed the following results: 108.9 for the 0.8 mm thick sheet, 115.3 for the 1 mm thick sheet, 117.6 for the 1.2 mm thick sheet in the S250 GD grades, while the 2 mm thick S350 GD grade had a hardness of 138.

The hardness of S250GD galvanized sheets varies depending on the thickness of the material, thus, thinner sheets have slightly lower hardness values, while the thicker ones can have slightly higher values due to the slightly different processing conditions.

Figure 9 shows that for all specimens, the hardness measured in HAZ is higher than that of the base materials. This increase is attributed to thermal exposure during the brazing process. Although the process operates at relatively low heat input, the parameters employed in the process induced localized thermal effects that slightly increase the hardness in the HAZ. This change is likely related to microstructural transformations caused by the thermodynamic drive of atoms at elevated temperatures, which leads to grain growth and possible phase changes.

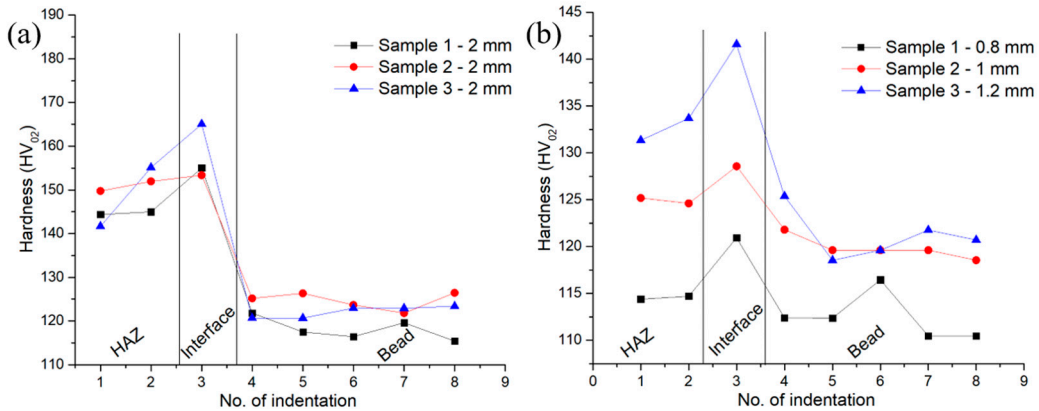

Figure 9. Hardness variation along Direction 1 at the interface between the 2 mm sheet and bead (**a**) and along Direction 2 at the interface between the thin sheets and bead (**b**).

In all samples, the interface shows the highest hardness values. The reason for this is that during brazing, an Fe–Al intermetallic layer with increased hardness is formed at

the base material/bead interface, and its evolution is governed by the interdiffusion of iron and aluminum atoms across the interface, as described by Singh et al. [13]. When the heat input is slightly increased, it can be seen that the hardness values of the bead increase as well due to the formation of a higher volume of intermetallics in the areas close to the interface. In the case of the 0.8 mm sheet, the observed lower hardness may be attributed to the reduced heat input during brazing, which likely limited the formation of intermetallic compounds in the investigated area.

The average hardness values calculated based on nine measurements performed in the center of the bead are shown and compared in Figure 10. The hardness is lower compared to that measured at the interface as a result of the absence of intermetallics in this area. Since the bead is a highly ductile alloy, there is no significant variation in hardness. The values are lower compared to those published by Basak et al., who obtained an alloy with a hardness of 180 HV in the fusion zone due to dispersion hardening when using $CuAl_8$ filler [11]. Besides, some lower values of about 155 HV were reported by Duarte et al. on forged $CuAl_8$ alloy due to the formation of precipitates [22].

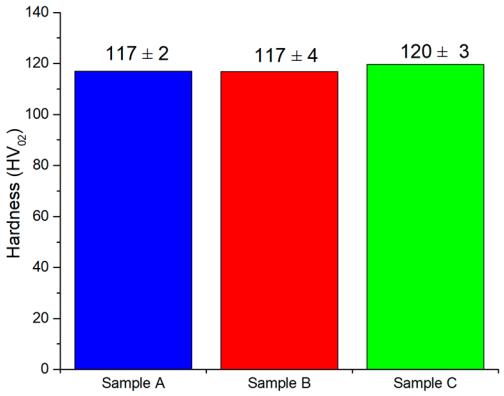

Figure 10. Hardness values measured in the center of the bead.

Based on the results presented in Figure 11, it can be observed that an improved joint strength was obtained using a heat input of 121.4 J/mm and sheets of 1.2 and 2 mm thickness used to prepare Specimen 3, which presented an increase in the yield strength. It can be assumed that joint efficiency is due to the increased heat input resulting in better wetting and increased cross-sectional area of the joint [9], along with the use of a thicker sheet.

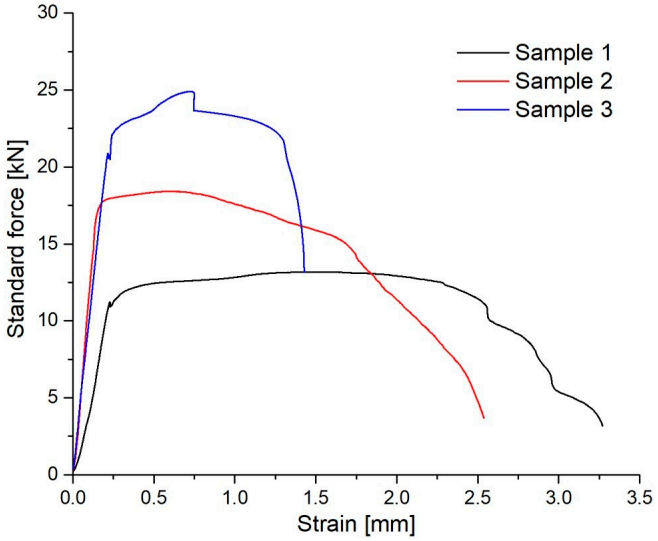

Figure 11. Force displacement curves of the lap-brazed samples.

The tests revealed two failure modes, as presented in Figure 12. For thinner sheets (0.8 and 1 mm thickness) the fracture occurred in the heat-affected zone close to the weld. On the other hand, in the case of the thicker sheet (1.2 mm thickness), a smooth ductile behavior can be noticed with failure in the base material at a distance of about 40 mm from the brazed joint with no fragile breakage in the HAZ. In the case of Specimens 1 and 2, it can be seen that the joints did not undergo any deterioration, but the fracture occurred in the HAZ. The heat input and overheating lead to embrittlement in the HAZ where the fracture occurred, most probably due to microstructural changes such as grain coarsening.

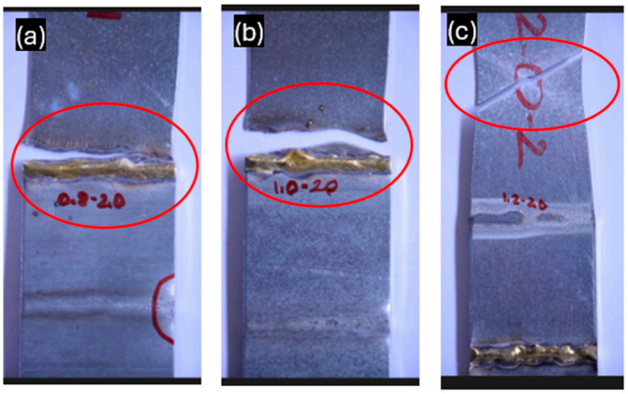

Figure 12. Failure modes of the tested specimens: fracture in the heat-affected zone (**a**,**b**) and fracture in the base material (**c**).

Grain size plays a crucial role in mechanical properties. Coarse grains often lead to a reduction in strength, plasticity, and toughness due to a relatively high number of dislocations and vacancies [23]. By enhancing heat dissipation in the base material when using a thicker sheet than 1 mm, it can be observed that the bead has enhanced resistance, making MIG brazing suitable for the construction of built-up beams.

4. Conclusions

This study proposed MIG brazing as a new joining solution for built-up cold-formed steel beams made of corrugated steel webs and flanges made of thin-walled cold-formed profiles using $CuAl_8$ wire as filler. Based on the macro- and microstructural observations and mechanical tests carried out in this work, the following conclusions can be drawn:

- The specimens exhibited a heterogeneous microstructure, with variations in the shape and size of the grains due to differences in the cooling rate. Specimen 1 presented randomly oriented elongated grains, suggesting fast directional cooling; Specimen 2 had a coarser structure characterized by elongated grains; Specimen 3 has a heterogeneous granular microstructure consisting mainly of equiaxed grains, which is the result of a slower cooling process.
- The microstructure at the interface of the bead reveals a complex formation of α-dendrites surrounded by eutectic material, with intermetallics formed due to the dissolution of Fe from the base material into the bead alongside very fine spherical precipitates. The formation of intermetallics is more pronounced near the base material, likely due to the higher affinity of iron for aluminum compared to copper.
- In all samples, the interface shows the highest hardness values. The reason for this is that during brazing, an Fe–Al intermetallic layer with increased hardness is formed at the base material/bead interface. Besides, when the heat input is slightly increased, it can be seen that the hardness values in the areas close to the interface increase as well due to the formation of a higher volume of intermetallics. Since no intermetallic

compounds are present at the center of the bead, there is no significant variation in hardness across this region.

- An improved joint strength was obtained using a heat input of 121.4 J/mm and sheets of 1.2 and 2 mm thickness, which showed an increase in yield strength. In this case, a smooth ductile behavior was observed with failure of the base material at a distance of approximately 45 mm from the brazed joint, without fragile fracture in the HAZ.

Author Contributions: Conceptualization, I.H. and V.U.; methodology, I.H and A.P (Alexandru Pascu); software, S.S. and A.P. (Alin Popescu); validation, V.U. and A.P. (Alexandru Pascu); formal analysis, I.H.; investigation, I.H., A.P. (Alexandru Pascu), S.S. and A.P. (Alin Popescu); resources, V.U.; data curation, writing—original draft preparation, I.H.; writing—review and editing, V.U. and A.P. (Alexandru Pascu); visualization, V.U.; supervision, I.H. and A.P. (Alexandru Pascu). All authors have read and agreed to the published version of the manuscript.

Funding: This research received no external funding.

Data Availability Statement: The data presented in this study are available on request from the corresponding author.

Conflicts of Interest: The authors declare no conflicts of interest.

References

1. Ungureanu, V.; Both, I.; Burca, M.; Radu, B.; Neagu, C.; Dubina, D. Experimental and numerical investigations on built-up cold-formed steel beams using resistance spot welding. *Thin-Walled Struct.* **2021**, *161*, 107456. [CrossRef]
2. Both, I.; Ungureanu, V.; Tunea, D.; Crisan, A.; Grosan, M. Experimental and Numerical Investigations on Cold-Formed Steel Beams Assembled by MIG Brazing. In Proceedings of the Eighth International Conference on Thin-Walled Structures—ICTWS, Lisbon, Portugal, 24–27 July 2018.
3. Dubina, D.; Ungureanu, V.; Gîlia, L. Thin-Walled Structures Experimental investigations of cold-formed steel beams of corrugated web and built-up section for flanges. *Thin-Walled Struct.* **2015**, *90*, 159–170. [CrossRef]
4. Tran, V.X.; Pan, J.; Pan, T. Fatigue behavior of spot friction welds in lap-shear and cross-tension specimens of dissimilar aluminum sheets. *Int. Fatigue J.* **2010**, *32*, 1022–1041. [CrossRef]
5. Basak, S.; Pal, T.K.; Shome, M.; Maity, J. GMA brazing of galvannealed interstitial-free steel. *Weld. J.* **2013**, *92*, 29–35.
6. Basak, S.; Das, H.; Pal, T.K.; Shome, M. Corrosion behaviour of MIG brazed and MIG welded joints of automotive DP600-GI steel sheet. *J. Mater. Eng. Perform.* **2016**, *25*, 5238–5251. [CrossRef]
7. Singh, J.; Arora, K.S.; Shukla, D.K. Dissimilar MIG-CMT weld-brazing of aluminium to steel: A review. *J. Alloys Compd.* **2019**, *783*, 753–764. [CrossRef]
8. Ye, Z.; Huang, J.; Gao, W.; Zhang, Y.; Cheng, Z.; Chen, S.; Yang, J. Microstructure and mechanical properties of 5052 aluminum alloy/mild steel butt joint achieved by MIG-TIG double-sided arc welding-brazing. *Mater. Des.* **2017**, *123*, 69–79. [CrossRef]
9. Ghahfarokhi, S.S.; Kalashami, A.G.; Zhang, S.; Anousheh, A.S.; Midawi, A.R.H.; Yasnogorodski, V.; Zhou, Y.N.; Benoit, M.J. Investigation of the Critical Factors Influencing Mechanical Properties and Failure Behavior in Weld-Brazed ZnAlMg Coated Steel. *Metall. Mater. Trans. A* **2025**, *56*, 618–639. [CrossRef]
10. Chovet, C.; Guiheux, S. Possibilities offered by MIG and TIG brazing of galvanized ultra high strength steels for automotive applications. *Metall. Ital.* **2006**, *7-8*, 47–54.
11. Basak, S.; Pal, T.K.; Shome, M. High-cycle fatigue behavior of MIG brazed galvanized DP600 steel sheet joint-effect of process parameters. *Int. J. Adv. Manuf. Technol.* **2016**, *82*, 1197–1211. [CrossRef]
12. Khan, M.S.; Cho, Y.; Zhang, S.; Goodwin, F.; Biro, E.; Zhou, Y.N. The Effect of Zinc Coating Type on the Morphology, Joint Geometry, and Mechanical Properties of Weld-Brazed Thin-Gauge Automotive Steel. *Metall. Mater. Trans. A* **2023**, *54*, 179–195. [CrossRef]
13. Singh, J.; Shehryar, M.; Oliveira, J.P.; Singh, K. Brazing of high-strength steels: Recent developments and challenges. *Manuf. J. Process.* **2024**, *115*, 289–309. [CrossRef]
14. Lee, K.B.; Oh, S.T. Development of durability enhancement technology for arc welding in advanced high strength steel (AHSS) chassis parts. *J. Weld. Join.* **2015**, *33*, 50–56.
15. Singh, J.; Singh, K.; Kumar, D. High cycle fatigue performance of cold metal transfer (CMT) brazed C-Mn-440 steel joints. *Int. J. Fatigue* **2020**, *137*, 105663. [CrossRef]

16. Sharma, A.; Lee, S.J.; Choi, D.Y.; Jung, J.P. Effect of brazing current and speed on the bead characteristics, microstructure, and mechanical properties of the arc brazed galvanized steel sheets. *J. Mater. Process. Technol.* **2017**, *249*, 212–220. [CrossRef]
17. Yu, Z.S.; Li, R.F.; Qi, K. Growth behavior of interfacial compounds in galvanized steel joints with CuSi3 filler under arc brazing. *Trans. Nonferrous Met. Soc. China* **2006**, *16*, 1391–1396. [CrossRef]
18. Reisgen, U.; Angerhausen, M.; Pipinikas, A.; Twiehaus, T.; Wesling, V.; Barthelmie, J. The effect of arc brazing process parameters on the microstructure and mechanical properties of high-strength steel HCT780XD using the copper-based filler metal CuAl8. *J. Mater. Process. Technol.* **2017**, *249*, 549–558. [CrossRef]
19. Dharmendra, C.; Shakerin, S.; Ram, G.J.; Mohammadi, M. Wire-arc additive manufacturing of nickel aluminum bronze/stainless steel hybrid parts–Interfacial characterization, prospects, and problems. *Materialia* **2020**, *13*, 100834. [CrossRef]
20. Singh, J.; Arora, K.S.; Shajan, N.; Shome, M.; Shukla, D.K. Influence of filler wire composition and heat input on microstructure and strength of CMT brazed DP steel joints. *Mater. Res. Express* **2019**, *6*, 116551. [CrossRef]
21. Hulka, I.; Radu, B.; Ungureanu, V.; Sîrbu, N.A. Microstructural Investigation and Mechanical Properties of Resistance Spot Welding Joints of Mild Steel Sheets. *Key Eng. Mater.* **2024**, *989*, 57–63. [CrossRef]
22. Duarte, V.R.; Rodrigues, T.A.; Schell, N.; Miranda, R.M.; Oliveira, J.P.; Santos, T.G. In-situ hot forging directed energy deposition-arc of CuAl8 alloy. *Addit. Manuf.* **2022**, *55*, 102847. [CrossRef]
23. Xu, Z.; Li, X.; Li, S.; Jiang, R.; Hua, P.; Liu, D. Wire arc additive manufacturing of CuAl8Ni2/42CrMo bimetallic deposition: Microstructure and properties. *J. Mater. Sci.* **2025**, *60*, 2623–2639. [CrossRef]